Cell

Cell-free Formation of RNA Granules: Bound RNAs Identify Features and Components of Cellular Assemblies

Tina W. Han,[1] Masato Kato,[1] Shanhai Xie,[1] Leeju C. Wu,[1] Hamid Mirzaei,[1] Jimin Pei,[3] Min Chen,[2] Yang Xie,[2] Jeffrey Allen,[2] Guanghua Xiao,[2] and Steven L. McKnight[1,*]
[1]Department of Biochemistry
[2]Department of Clinical Sciences
[3]Howard Hughes Medical Institute
UT Southwestern Medical Center, 5323 Harry Hines Boulevard, Dallas, TX 75390-9152, USA
*Correspondence: steven.mcknight@utsouthwestern.edu
DOI 10.1016/j.cell.2012.04.016

SUMMARY

Cellular granules lacking boundary membranes harbor RNAs and their associated proteins and play diverse roles controlling the timing and location of protein synthesis. Formation of such granules was emulated by treatment of mouse brain extracts and human cell lysates with a biotinylated isoxazole (b-isox) chemical. Deep sequencing of the associated RNAs revealed an enrichment for mRNAs known to be recruited to neuronal granules used for dendritic transport and localized translation at synapses. Precipitated mRNAs contain extended 3′ UTR sequences and an enrichment in binding sites for known granule-associated proteins. Hydrogels composed of the low complexity (LC) sequence domain of FUS recruited and retained the same mRNAs as were selectively precipitated by the b-isox chemical. Phosphorylation of the LC domain of FUS prevented hydrogel retention, offering a conceptual means of dynamic, signal-dependent control of RNA granule assembly.

INTRODUCTION

Asymmetric localization of mRNAs is a process used by cells to restrict protein synthesis to specific subcellular domains. This mechanism of RNA regulation is important for diverse biological processes including segregation of cell fate determinants, specification of cell polarity, and synaptic plasticity. For example, uneven distribution of maternal RNAs in the oocytes of the fruit fly, *Drosophila melanogaster,* facilitates the asymmetric distribution of cytoplasmic determinants into germline precursor cells and the establishment of morphogen gradients required for axial patterning (Palacios and St Johnston, 2001). Accumulation of β-actin mRNA in the leading edges of chick embryonic fibroblasts has been shown to direct the sites of actin polymerization that drive cell migration (Kislauskis et al., 1993; Kislauskis et al., 1994). β-actin mRNA is also transported to the tips of growth cones in developing axons seeking synaptic connections (Zhang et al., 2001). Active transport of specialized RNAs to neuronal processes for localized translation at or near synapses has been implicated in the modulation of synaptic plasticity. One of the best-characterized dendritically targeted mRNAs in mammals is the transcript encoding calcium/calmodulin-dependent protein kinase II alpha or CamkIIα (Burgin et al., 1990). Mice tailored to express an aberrant version of the mRNA encoding CamkIIα, wherein the 3′ untranslated (3′ UTR) was modified to retain the mRNA in nerve cell soma and suffer significant reductions in long-term potentiation (LTP) as well as deficits in hippocampus-dependent spatial memory tasks (Miller et al., 2002).

In many instances, RNA transcripts are packaged into ribonucleoprotein (RNP) aggregates, called RNA granules, for transport to specific sites in the cytoplasm to facilitate localized translation. RNA granules are electron-dense, nonmembrane delimited organelles that have been observed in diverse biological contexts (Mahowald, 1962; Nover et al., 1983; Knowles et al., 1996). They were first observed in the early 1900s by the American zoologist, Robert Hegner, as dark puncta enriched in the posterior pole of chrysomelid beetle eggs. Ablation of posterior pole plasm with a hot needle subsequently abolished germ line development in the beetle embryo (Hegner, 1908; Hegner, 1911). Granule-associated plasm was further established as germline determinants with transplantation experiments in the early 1970s that demonstrated rescue of germ cell formation in UV-irradiated fly embryos (Illmensee and Mahowald, 1974; Okada et al., 1974).

Heretofore it has been difficult to reconstitute cell-free assembly assays of RNA granules that might be valuable for understanding how certain mRNAs are chosen for localized subcellular transport. As such, it has been problematic to conceptualize how mRNAs are dynamically assembled into RNA granules in one part of a cell, yet released for localized translation in another cellular compartment. Here we report the results of studies aimed to resolve the properties of mRNAs that are recruited into RNA granule-like aggregates precipitated by microcrystals of a biotinylated isoxazole (b-isox) chemical, or recruited into hydrogel droplets composed of polymerized

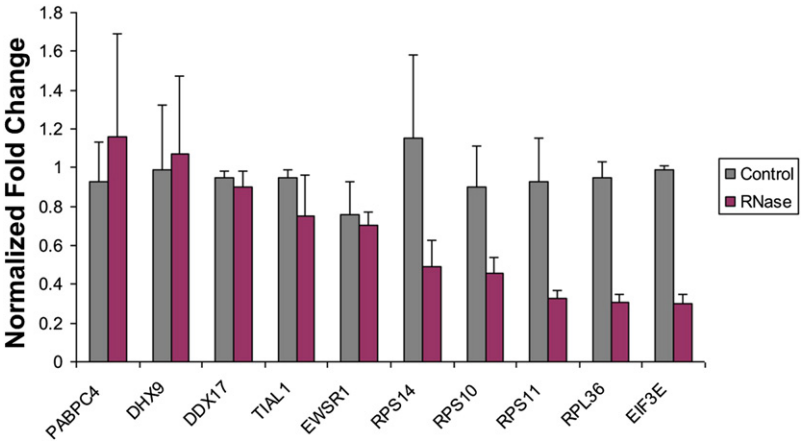

Figure 1. Isoxazole-Mediated Precipitation Is Partially Sensitive to RNase

SILAC mass spectrometry was used to quantify changes in protein precipitation by b-isox following RNase treatment of U2OS cell lysate. Normalized fold change is shown for five representative proteins that precipitate irrespective of RNase treatment alongside five representative proteins whose precipitation by b-isox decreases as a function of RNase treatment. Error bars are standard deviation of triplicate experiments. See also Table S1.

fibers of low complexity sequences derived from RNA-binding proteins. The results of these studies offer a conceptually simple model describing the molecular determinants of RNA granule assembly and disassembly.

RESULTS

Two sources of materials were employed to investigate whether RNAs might be selectively precipitated by the biotinylated isoxazole (b-isox) chemical to form RNA granule-like aggregates in cell-free reactions. One source was lysate prepared from adult mouse brain tissue, the other was lysate prepared from human U2OS cells. Because human cells had not been evaluated in the accompanying study (Kato et al., 2012, this issue of *Cell*), we initially utilized mass spectrometric methods to analyze the human proteins precipitated upon exposure of U2OS lysates to a 100 μM concentration of the b-isox chemical. The list of human proteins precipitated by the compound overlapped extensively with the mouse and fruit fly proteins described in the accompanying manuscript. Of the 237 proteins identified by mass spectrometry in the b-isox precipitate of U2OS lysate, the vast majority were RNA-binding proteins, RNA helicases, translation factors, poly-A-binding proteins, mRNA cap-binding proteins, and ribosomal proteins. We thereby conclude that the b-isox chemical perturbs the lysate prepared from human U2OS cells in a manner similar to its effects on lysates prepared from mouse cell lines, mouse tissues, and *Drosophila melanogaster* S2 cells.

Low Complexity Proteins Are Not Dependent on RNA for Recruitment to Granule-Like Aggregates

As we began to consider studies of the RNA components of RNA granule-like aggregates formed in test tube reactions, we initially wondered whether the b-isox compound would cause precipitation in samples that had been subjected to treatment with RNase. U2OS lysates were prepared from cells that had been grown in defined tissue culture medium supplemented with either regular lysine (light) or heavy isotope-containing lysine. The latter lysate was subjected to RNase treatment, and then both samples were individually incubated with the b-isox chemical. Precipitated materials were recovered by centrifugation, mixed, and then subjected to stable isotope labeling with amino acids in cell culture (SILAC) mass spectrometry. Both samples contained the same distribution of proteins associated with RNA biogenesis as had been observed with the human, mouse, and fly samples analyzed earlier. Quantitative inspection of the data revealed two categories of proteins, one consisting of polypeptides that were observed at equivalent levels in the heavy and light precipitates and another consisting of proteins that were observed at a reduced abundance in the sample that had been treated with RNase prior to b-isox-mediated precipitation. The former category was typified by hnRNP proteins containing KH domains, RRM domains, and low complexity (LC) sequence domains. The latter category was typified by ribosomal proteins and translation initiation factors that were largely devoid of LC sequences. Figure 1 shows five representative samples of proteins that were precipitated equivalently irrespective of RNase treatment, as well as five representative proteins that were precipitated less effectively subsequent to RNase degradation of the lysate. Both lists of proteins were quantitatively compared and can be found in Table S1, available online.

Computational analyses were undertaken to score for the density of LC sequences in the aforementioned categories of proteins. As demonstrated by Kato and colleagues (Kato et al., 2012), the lists of proteins precipitated by the b-isox chemical from mouse brain and testis tissue, mouse ES and NIH 3T3 cells, and *Drosophila* S2 cells were highly enriched in LC sequences. When this same method of analysis was applied to the two categories of proteins emerging from the SILAC experiment described above, it was observed that proteins that were precipitated equivalently irrespective of RNase treatment remained enriched in LC sequences. By computational definition, 12% of the polypeptides in the human proteome contain an LC domain (Experimental Procedures). Of the list of proteins precipitated by the b-isox chemical prior to RNase treatment, 29% contained LC domains. An even higher percentage of the list of proteins precipitated irrespective of RNase treatment, 38%, contained LC domains. By contrast, proteins that were precipitated at a diminished level following RNase treatment—including ribosomal proteins and translation factors—were not statistically enriched in LC sequences.

Analysis of RNAs Precipitated by the Biotinylated Isoxazole

Lysates prepared from mouse brain tissue and cultured U2OS cells were exposed to a 100 μM concentration of the b-isox

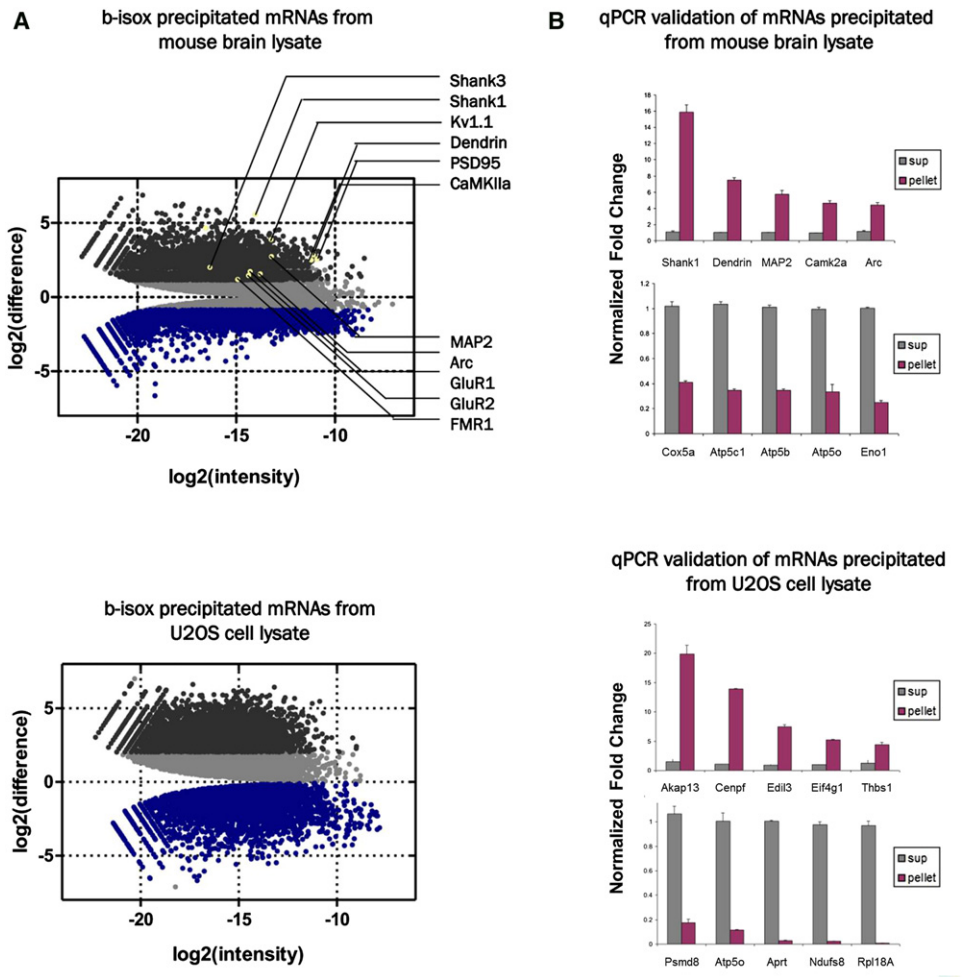

Figure 2. Isoxazole-Mediated Precipitation of mRNAs

(A) RNA-Seq plots for mRNAs that partition to either the b-isox pellet or remain in the supernatant from mouse brain lysate (top panel) and human U2OS cell lysate (bottom panel). Relative abundance of the transcript in the cell is plotted on the x axis in $\log_2$ scale and fold enrichment of the transcript in the b-isox precipitant (the pellet to supernatant ratio) is plotted on the y axis in $\log_2$ scale. Shaded in dark gray are mRNAs more than 2-fold enriched in the pellet and shaded in blue are mRNAs that are 2-fold or greater excluded from the pellet. Eleven known dendritic RNAs are highlighted in the mouse brain data set. See also Tables S2 and S3.

(B) Quantitative validation by qPCR for five representative mRNAs enriched in the pellet and five representative mRNAs retained in supernatant precipitated from mouse brain lysate (top panel) and U2OS cell lysate (bottom panel). Normalized fold change (pellet to supernatant ratio) is plotted and error is standard deviation of triplicate experiments.

compound. Precipitated materials were recovered by centrifugation, washed, and used to prepare poly-A+ mRNA for deep sequencing (Extended Experimental Procedures and Table S2). In addition to sequencing the precipitated fraction of mRNAs, we also performed deep sequencing on poly-A+ mRNAs that were left in the supernatant fraction. Figure 2A shows the distribution of mouse brain mRNAs and human U2OS mRNAs that partitioned to either the precipitate or supernatant fraction. Confirmatory qPCR assays were performed on ten mRNAs from each sample, including five that were selectively precipitated and five that were left in the supernatant (Figure 2B). Literature publications on mRNAs that are believed to enter neuronal granules for dendritic translocation have highlighted 11 gene products, including the mRNAs encoding Camk2a, MAP2, Arc, Shank1, Shank3, GluR1, GluR2, FMR1, Kv1.1, PSD95, and dendrin (Böckers et al., 2004; Burgin et al., 1990; Caceres et al., 1983; Feng et al., 1997; Grooms et al., 2006; Herb et al., 1997; Link et al., 1995; Lyford et al., 1995; Muddashetty et al., 2007; Wang et al., 1994) Encouragingly, the mRNAs encoding all 11 of these proteins were observed to be enriched by b-isox precipitation (Figure 2A).

What features distinguish mRNAs precipitated by the b-isox chemical relative to ones left in the supernatant? Prominent distinctions were initially observed when computationally comparing the lists of precipitated and soluble mRNAs in gene ontology (GO) programs (Experimental Procedures). The top two GO categories for mRNAs precipitated from the U2OS lysates were cell adhesion and axon guidance. By contrast, the mRNAs left in the supernatant highlighted mitochondrial electron transport, respiratory electron transport chain, and regulation of

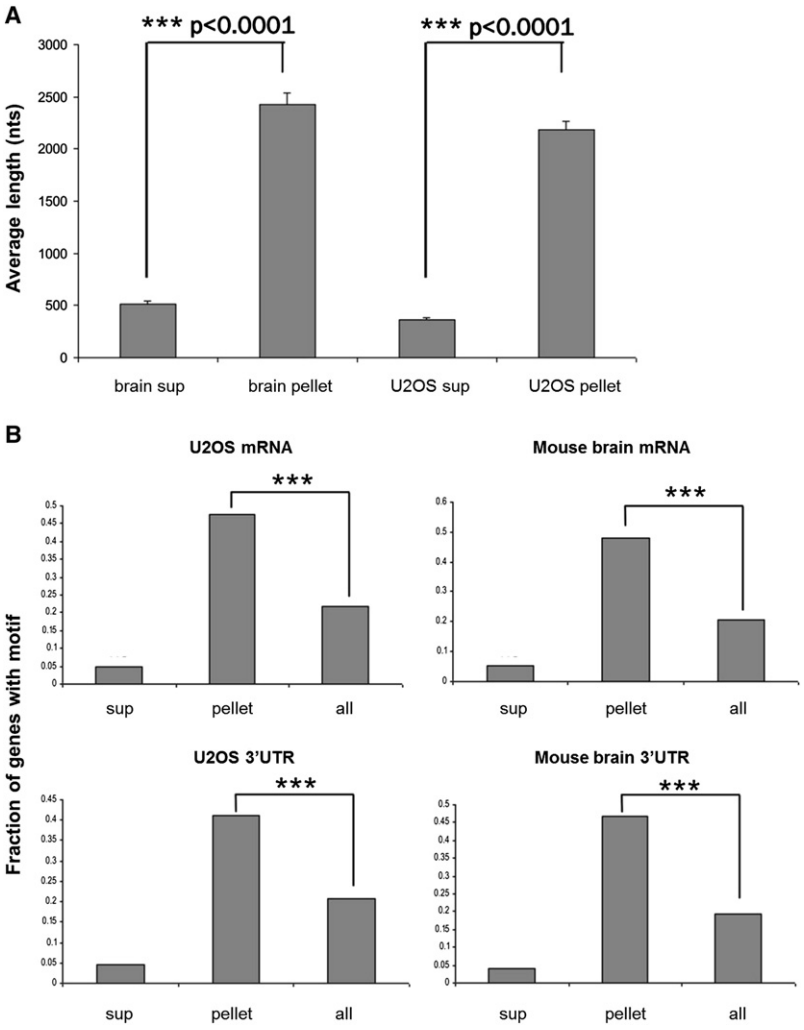

Figure 3. Analysis of 3′ UTR Lengths in Supernatant and Pellet mRNAs

(A) Pellet-enriched 3′ UTRs from both mouse brain and U2OS RNA-Seq data sets are longer than supernatant-retained 3′ UTRs. The average 3′ UTR length in nucleotides is compared here. Error bars are ± standard error of the mean and ***p value < 0.0001 by Mann-Whitney test.

(B) Computational analysis of the consensus pumilio-binding motif 5′-UGUANAUA-3′ in supernatant- and pellet-enriched mRNAs (top panels) and analysis of motifs in 3′ UTRs only (bottom panels) in both mouse brain and U2OS data sets. Fraction of RNAs with pumilio motif is significantly enriched in pellet mRNAs and 3′ UTRs compared to supernatant mRNAs and 3′ UTRs in both U2OS and mouse brain RNA-Seq data sets. ***p value < 2.2×10^{-16} by Fisher's exact test.

cellular amino acid metabolic processes. For the mRNAs precipitated from the mouse brain lysate, GO categories highlighted regulation of transcription, axon guidance, synaptic transmission, and myelination in the peripheral nervous system. As in the case of U2OS cells, mRNAs excluded from b-isox precipitation from the mouse brain lysate highlighted GO categories including electron transport chain, oxidation reduction and metabolic processes (Table S3). Although categorization attempts via gene ontology are of limited acuity, it does appear that certain aspects of cellular function—such as mitochondrial processes—can be linked to mRNAs excluded from b-isox-mediated precipitation, whereas others—such as cell adhesion and axonal/dendritic/synaptic functions are associated with b-isox-precipitated mRNAs.

A second striking difference between soluble and b-isox precipitated mRNA was the average 3′ UTR length. In the data set gathered from mouse brain tissue, mRNAs enriched by b-isox precipitation exhibited an average 3′ UTR length (2.43 ± 0.10 kB) roughly 5-fold longer than that of mRNAs excluded from the precipitate (0.51 ± 0.03 kB). This same discrepancy was observed from the U2OS data set. mRNAs precipitated by the b-isox chemical exhibited an average 3′ UTR length of 2.18 ± 0.81 kB, roughly 6-fold greater than the 0.368 ± 0.02 kB average for mRNAs left in the supernatant (Figure 3A).

One of the RNA-binding proteins present in the b-isox precipitates derived from human, mouse, and fruit fly samples is the pumilio protein. Flies encode a single pumilio protein, and mammals encode two paralogous versions of this RNA-binding protein (Pum1 and Pum2). Pumilio proteins bind to the nanos response element (NRE) in the 3′ UTR of mRNAs via their pumilio and FBF (PUF) domains (Murata and Wharton, 1995).The PUF domain, located toward the C termini of pumilio proteins, is composed of eight tandem, imperfect repeats of 36 amino acids that self-organize to form the RNA-binding domain (Zamore et al., 1997; Zhang et al., 1997). Pumilio proteins also contain LC sequences composed of poly-glutamine and poly-alanine segments located on the N-terminal side of the RNA-binding domain. Mouse strains carrying inactivating mutations in both alleles of the Pum2 gene have been reported to suffer deficits in dendrite maturation and morphology, consistent with the idea that pumilio proteins play an important role in the dendritic transport of selected mRNAs (Vessey et al., 2010).

Having observed that the fly pumilio protein was present in the b-isox precipitate of *Drosophila* S2 cells and that both Pum1 and Pum2 were precipitated in lysates prepared from human U2OS cells, mouse brain and testis tissue, and mouse ES cells, we performed a computational search for the canonical NRE sequence, 5′-UGUANAUA-3′, in the 3′ UTRs of mRNA samples that were either precipitated by the b-isox compound or left in the supernatant fraction. mRNAs harboring the canonical NRE sequence were found at a roughly 10× enhanced frequency in the b-isox precipitated mRNAs compared with those left in the supernatant in both mouse brain and U2OS derived data sets (Figure 3B and Experimental Procedures). The same enrichment was found when the computational search was restricted to the 3′ UTRs of the precipitated RNAs compared with supernatant RNAs, thereby indicating that most of the

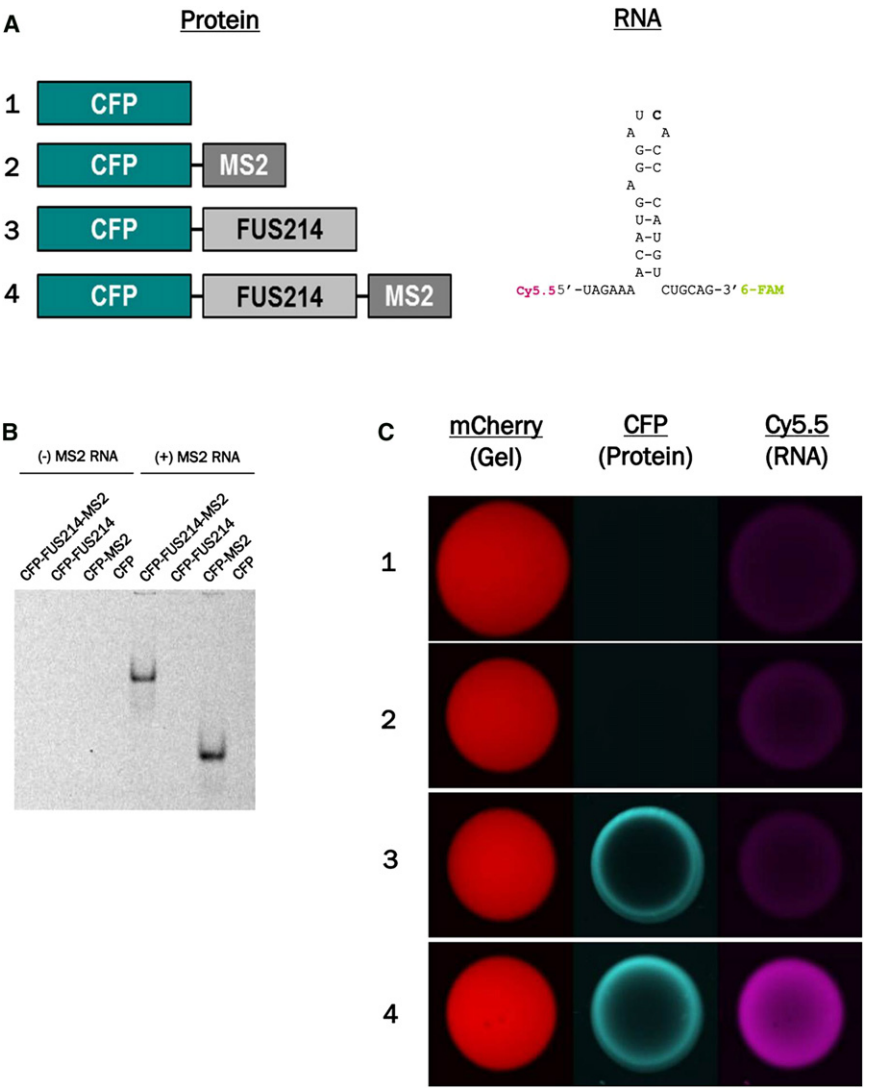

Figure 4. Gel Retention of RNA Is Codependent on Both RNA-Binding and LC Domains

(A) Chimeric proteins used for gel retention experiment are recombinant His-tagged proteins purified from bacteria (diagram is approximately to scale). RNA hairpin that is a high affinity substrate of the MS2 RNA-binding domain was synthesized with either 3′ 6-FAM (used for gel shift) or 5′ Cy5.5 (gel retention).

(B) Gel shift demonstrates binding of 6-FAM-labeled MS2 RNA hairpin to fusion proteins with MS2 RNA-binding domain. CFP alone and CFP-tagged FUS214 LC sequence do not interact with the MS2 RNA hairpin.

(C) Gel retention assay performed with both CFP-tagged protein and Cy5.5-labeled hairpin RNA. The MS2 RNA hairpin is only recruited into the hydrogel when incubated with CFP-FUS214-MS2, which contains both the capacity for binding RNA as well as LC elements required for gel retention. Lacking LC elements, CFP and CFP-MS2 do not accumulate in mCherry-FUS gel. CFP-FUS214 is retained by the gel but lacks the MS2 RNA-binding domain required for interaction with the MS2 RNA.

NREs found in the pelleted mRNAs are located in their 3′ UTRs (Figure 3B).

A Two Component Model Defines Selective Targeting of mRNAs to RNA Granules

Many of the RNA-binding proteins directly precipitated by the b-isox chemical consist of two definable functional domains. One such domain, which can be represented in multiple copies, is that required for the RNA-binding protein to directly recognize its mRNA target. These are typified by RNA recognition motif (RRM) domains, K-homology (KH) domains, double-stranded RNA-binding domains (dsRBDs), and PUF domains prototypical of mRNA-specific RNA-binding proteins. The second functionality commonly found in RNA-binding proteins precipitated by the b-isox chemical was represented by LC sequences that are capable of transitioning between soluble and polymeric states (Kato et al., 2012). We hypothesize that these LC sequences represent the determinant of RNA-binding proteins that allow dynamic entry into and out of RNA granules.

In order to test this two component model in the complete absence of the b-isox chemical, we prepared and studied chimeric proteins composed of any of three polypeptide segments. One segment encoded the cyan fluorescent protein (CFP), a second component encoded the LC domain of FUS, and the third component encoded the RNA-binding domain of the MS2 phage coat protein (Figure 4A). Chimeric proteins composed of one, two, or all three domains were incubated with a fluorescently modified version of the RNA hairpin known to bind avidly to the MS2 coat protein (Bernardi and Spahr, 1972). As assayed by gel mobility shift experiments, the two chimeric proteins containing the MS2 RNA-binding domain were observed to bind to the fluorescently tagged hairpin RNA (Figure 4B). When the various proteins were exposed to mCherry:FUS hydrogel droplets, in combination with the fluorescently tagged hairpin RNA, hydrogel retention of the RNA was only observed with the protein containing CFP, the LC domain of FUS, and the MS2 RNA-binding domain (Figure 4C). We hypothesize that the fluorescently labeled hairpin RNA binds to the MS2 RNA-binding domain and that the LC domain of FUS then facilitates hydrogel retention via its polymeric incorporation into the fibrous core of the mCherry:FUS hydrogel. Retention of the hairpin RNA in the hydrogel droplet is interpreted to take place only if both of these reactions are satisfied.

FUS Hydrogel Droplets Recruit the Same mRNAs as Those Precipitated by the Biotinylated Isoxazole

Knowing that hydrogel droplets formed upon concentration of the chimeric protein consisting of mCherry linked to the low

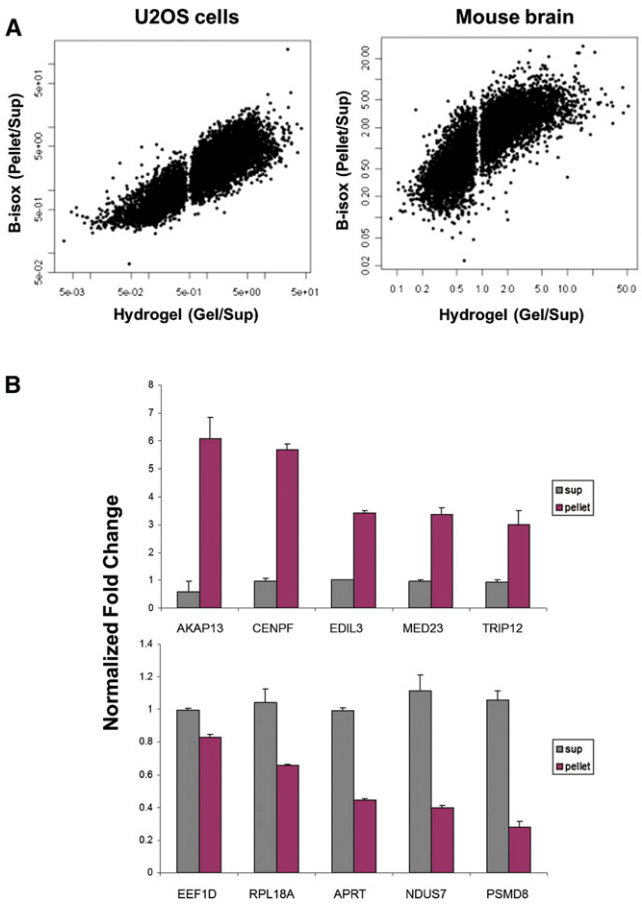

Figure 5. Gel Retention of mRNAs from Cell Lysate Correlates with Isoxazole-Precipitated mRNAs

(A) RNA-Seq data from gel retained RNAs were compared to RNA-Seq data from isoxazole precipitated RNAs with gel-to-supernatant ratio graphed on x axis and b-isox pellet to supernatant ratio graphed on the y axis for every RNA with an RPKM value > 1. High degree of concordance was found between these two data sets: U2OS cells (correlation = 0.86, p value < 2×10^{-16}) and mouse brain (correlation = 0.79, p value < 2×10^{-16}). See also Table S4.

(B) qPCR validation for five representative mRNAs enriched in the hydrogel (top) and five representative mRNAs that were retained in the supernatant from U2OS cell lysate (bottom). Data are plotted as normalized fold change and error is standard deviation of triplicate experiments.

complexity (LC) domain of FUS are able to capture and retain GFP hybrids linked to the LC domains of heterotypic RNA-binding proteins (Kato et al., 2012), we wondered whether it might be possible that these droplets could selectively capture mRNPs present in the lysates of mouse brain tissue and U2OS cells. Larger mCherry:FUS droplets, preformed on Parafilm, were incubated with lysate and processed for the production of mRNA to be analyzed by deep sequencing (Table S4). RNA was also processed from the supernatant to identify mRNAs not recruited into the mCherry:FUS hydrogel droplets.

As shown in Figure 5A, the mCherry:FUS droplets captured virtually the same mRNAs from both mouse brain tissue and U2OS cell lysates as were precipitated by the b-isox chemical. Likewise, the same mRNAs that failed to be precipitated by the b-isox chemical also failed to be captured by the mCherry:FUS hydrogel droplets. Indeed, the degree of over- or underrepresentation of individual mRNAs in the two data sets matched so well as to yield a level of statistical significance that exceeded the < 2×10^{-16} limit of the computational algorithm that was applied to compare the two data sets (Experimental Procedures). The observations reported by Kato and colleagues (Kato et al., 2012) provided evidence that the LC domains of a number of different RNA-binding proteins could be captured and retained by the mCherry:FUS hydrogel. We hypothesize that these same RNA-binding proteins, when associated with the 3′ UTRs of their mRNA targets, utilize their LC sequences to "address" their target mRNAs into the mCherry:FUS hydrogel.

A Computational Strategy to Define Networks of Interaction between Distinct RNA-Binding Proteins and Their mRNAs Targets

Given the simplicity and reproducibility in assigning the identities of mRNAs precipitated by the b-isox chemical, or trapped by mCherry:FUS hydrogel droplets, we sought to determine whether these methods might be of utility in identifying the mRNA targets of specific hnRNP proteins. shRNA reagents were prepared so as to allow the selective reduction of the mRNA and protein products of the genes encoding FUS and its closest paralog, EWS (Experimental Procedures). U2OS cells infected with a lentivirus construct expressing the shRNA specific to FUS revealed mRNA reduction of roughly 70% as compared to control (Figure 6A). Perplexingly, the cells exposed to shRNA-mediated reduction of FUS revealed a modest increase in the expression of the EWS protein. Cells infected with the lentivirus construct expressing the shRNA specific to EWS revealed mRNA reduction by roughly 85%, with no concomitant change in expression of the FUS mRNA. Cells infected by both lentiviruses exhibited roughly 80% reduction in FUS mRNA and 90% reduction in EWS mRNA. Qualitative confirmation of these knockdown experiments were obtained by western blotting (Figure 6A).

Samples were prepared from cells infected with an inert lentivirus, as well as cells exposed to lentiviruses expressing FUS-specific shRNA, EWS-specific shRNA, or both. The four lysates were incubated on ice with 100 μM of the b-isox chemical, allowing retrieval and deep sequencing of the precipitated RNA (Table S5). As shown in Figure 6D, computational analysis of the resulting data revealed 283 mRNAs that were at least 2× underrepresented in the sample prepared from U2OS cells in which both FUS and EWS were knocked down (relative to the sample prepared from cells exposed to the inert virus). In the FUS-only knockdown sample, 50 RNAs were at least 2× underrepresented relative to the control (Figure 6B). Encouragingly, 41 of these mRNAs were present in the set of 283 mRNAs deemed to be significantly underrepresented in the double knockdown sample (Figure 6D). Twenty mRNAs were observed to be at least 2× underrepresented in the sample prepared from cells in which the level of EWS had been attenuated by shRNA knockdown (Figure 6C). Seventeen of these mRNA species were represented in the double knockdown sample, yet only 5 were present in the list of 50 mRNAs underrepresented in the FUS-only knockdown sample.

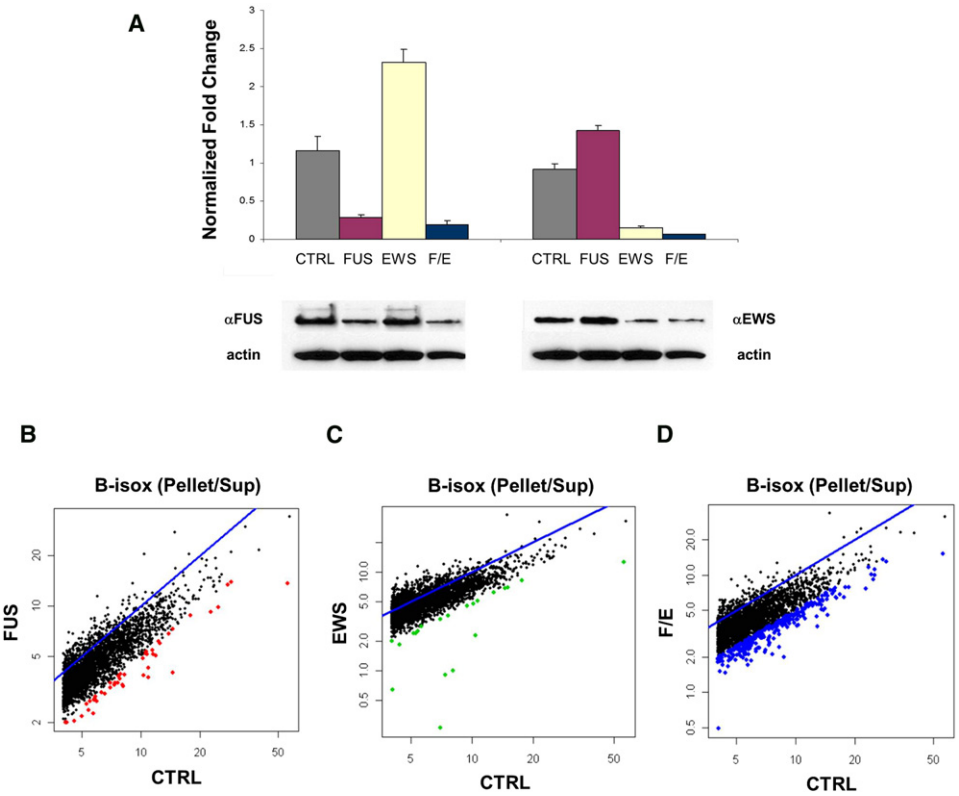

Figure 6. Precipitation of mRNAs Following Knockdown of FUS, EWS, or Both in U2OS Cells

(A) The efficiency of shRNA-mediated knockdown of FUS and EWS in U2OS cells was confirmed by both qPCR and western blot analysis. U2OS cells were infected with lentivirus bearing shRNA specific to either FUS, EWS, or both. FUS-only knockdown cells exhibited an mRNA reduction of roughly 70% relative to cells infected with an inert virus. EWS-only knockdown cells exhibited an mRNA reduction of roughly 85% relative to control cells. Under double knockdown conditions, mRNA levels of FUS and EWS were reduced to 80% and 90%, respectively, as compared with control. The error bars are standard deviation of triplicate experiments.

(B) RNA-Seq was performed on both RNAs precipitated by b-isox from knockdown cell lysate and RNAs remaining in the supernatant. This scatterplot shows the RNA-Seq data from the single FUS knockdown with control pellet/sup ratio graphed on the x axis and FUS knockdown pellet/sup ratio on the y axis. The blue line signifies that the ratio between knockdown and control is 1 or no change. Data points highlighted in red indicate RNAs that exhibit at least a 2-fold reduction in precipitation as a function of FUS knockdown. See also Table S5.

(C) RNA-Seq data from the single EWS knockdown with control pellet/sup ratio graphed on the x axis and EWS knockdown pellet/sup ratio on the y axis. Data points highlighted in green indicate RNAs that exhibited at least a 2-fold reduction in precipitation as a function of EWS knockdown.

(D) RNA-Seq data from the double FUS/EWS knockdown with control pellet/sup ratio graphed on the x axis and FUS/EWS knockdown pellet/sup ratio on the y axis. Data points highlighted in blue indicate RNAs that exhibit at least a 2-fold reduction in precipitation as a function of double FUS/EWS knockdown.

The statistical probability of 41 mRNAs underrepresented in the FUS-only knockdown sample being present in the list of 283 mRNAs underrepresented in the double knockdown sample revealed a p value of $< 2.2 \times 10^{-16}$. Significant statistical significance was also attributable to the fact that 17 mRNAs underrepresented in the EWS-only knockdown were found in the double knockdown list. We hypothesize that the mRNAs observed to be underrepresented in both of the dual sample sets (FUS-only plus FUS:EWS, and EWS-only plus FUS:EWS) represent mRNAs that depend heavily on either FUS or EWS to be precipitated into the b-isox precipitate. As will be discussed subsequently, these mRNAs were, at an exceptional level of statistical significance, found to be included in a recently published data set of mRNAs assigned by PAR-CLIP as direct targets of either FUS or EWS (Hoell et al., 2011).

Phosphorylation of the LC Domain of FUS Impedes Retention to the mCherry:Fus Hydrogel

The highly dynamic behavior of RNA granules in cells suggests that assembly/disassembly might be a regulated process. An unbiased screen for substrates for DNA-dependent protein kinase (DNA-PK) led to the discovery of FUS as a DNA-PK substrate (Gardiner et al., 2008). By mapping the precise sites of phosphorylation, Gardiner and colleagues found that DNA-PK phosphorylates serine residues located on the immediate, C-terminal side of three of the [G/S]Y[G/S] motifs located within the LC domain of FUS. In order to test whether DNA-PK-mediated phosphorylation of FUS might affect its ability to bind to the mCherry:FUS hydrogel, recombinant DNA-PK was incubated in the presence of [γ-^{32}P]-labeled ATP with the chimeric protein linking GFP to the LC domain of FUS. Dose-dependent

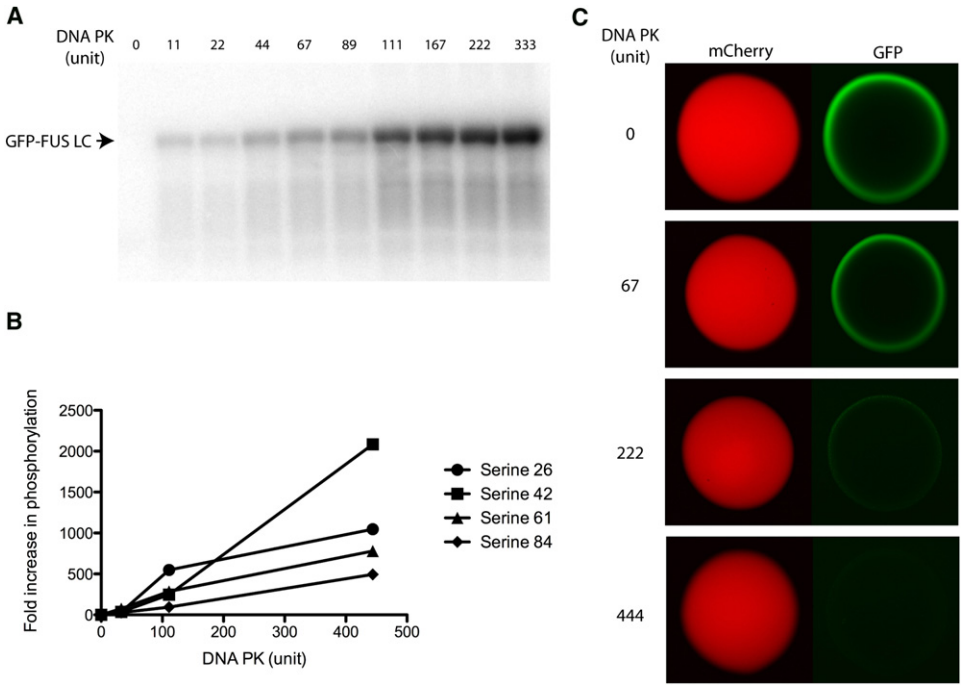

Figure 7. Inhibition of FUS LC Domain Hydrogel Binding by Phosphorylation

(A) The fusion protein linking GFP to the intact LC domain of FUS LC was phosphorylated by different units of DNA-dependent protein kinase (DNA-PK) in the presence of [γ-^{32}P] ATP. Phosphorylated protein samples were separated on SDS-PAGE followed by autoradiograph imaging.

(B) Sites of phosphorylation within the LC domain of FUS, as well as relative degrees of phosphorylation by DNA-PK, were determined by quantitative mass spectrometry (Experimental Procedures).

(C) The fusion protein linking GFP to the intact LC domain of FUS was phosphorylated by DNA-PK using unlabeled ATP (Experimental Procedures). Differentially phosphorylated samples were then applied to mCherry:FUS hydrogel droplets in order to test for gel trapping. The level of gel retention was observed to inversely correlate with the degree of DNA-PK-mediated phosphorylation.

phosphorylation was observed both by gel electrophoresis followed by autoradiography (Figure 7A) and proteomic analysis (Figure 7B). Proteomic analyses confirmed the sites of DNA-PK-mediated phosphorylation to serine residues 26, 42, 61, and 84, and quantitation of phosphorylation levels revealed proportional increases as a function amount of DNA-PK added to each reaction (Experimental Procedures). Incubation of differentially phosphorylated derivatives of GFP:FUS with mCherry:FUS hydrogel droplets gave evidence that phosphorylation impedes hydrogel retention of the test protein. Partially phosphorylated preparations of GFP:FUS bound to the droplets with qualitatively reduced avidity compared with the unmodified protein, and extensively phosphorylated samples bound to the hydrogel no better than GFP alone (Figure 7C). Whereas these experiments do not speak to the biological relationship between FUS phosphorylation and its ability to associate with stress granules, they do show that it is formally possible that posttranslational modifications of the LC domain of FUS could be used to regulate its propensity to remain soluble or phase transition into a hydrogel-like state.

DISCUSSION

Together with the accompanying manuscript (Kato et al., 2012), this study reports observations enabled by our ability to recapitulate the cell-free formation of a precipitate bearing similarities to RNA granules. Kato and colleagues (Kato et al., 2012) have studied the protein constituents of the precipitate. The present manuscript is focused on the RNA constituents of the precipitate.

Initial experiments used deep sequencing methods to categorize the RNA species selectively precipitated or left soluble following exposure of mouse brain or human U2OS lysates to the biotinylated isoxazole (b-isox) chemical. Three observations indicated that the b-isox precipitate enriched retention of RNAs known to be associated with RNA granules. First, all of 11 distinct mRNAs known to be transported along dendrites via neuronal granules were enriched in the b-isox precipitate (Böckers et al., 2004; Bramham and Wells, 2007; Kislauskis et al., 1994; Kuhl and Skehel, 1998; Wang et al., 1994). Second, the 3′ UTRs of mRNAs selectively precipitated by the b-isox chemical were observed to be significantly longer than those of mRNAs left in the supernatant and contained a significantly enhanced frequency of binding sites for the pumilio mRNA-binding protein. This RNA regulatory protein was found as a protein constituent of the b-isox precipitates derived from fly, mouse, and human sources (Kato et al., 2012), and extensive genetic data have implicated pumilio in the functioning of RNA granules in *Drosophila* embryos and mammalian neurons (Lehmann and Nusslein-Volhard, 1987; Ye et al., 2004; Vessey et al., 2010).

Third, computational analyses of the mRNA that partitioned to the b-isox pellet highlighted gene ontology categories attributable to cellular functions anticipated to be dependent upon localized translation, including synapse formation and function. In combination, these observations provide evidence that the b-isox compound is not only selective in the protein species that it precipitates (Kato et al., 2012) but also exhibits selectivity in its ability to precipitate mRNA species known to be associated with RNA granules.

By treating lysates with RNase prior to exposure to the b-isox chemical, it was observed that RNA is not required for the precipitation of many of the proteins associated with RNA biogenesis. In retrospect, this is not surprising. The b-isox chemical selectively precipitates purified, recombinant RNA-binding proteins so long as they contain LC sequences (Kato et al., 2012). By using sensitive SILAC methods for quantitative proteomic analysis, we observed that RNase treatment attenuated the precipitation of certain categories of proteins associated with RNA biogenesis but not others. Prototypical examples of the former category are ribosomal proteins and translation factors. These proteins are not adorned with LC sequences, and we hypothesize that they are indirectly recruited into the b-isox precipitate by virtue of their association with the mRNPs that are selectively precipitated. RNase hydrolysis would obviously be expected to sever this relationship. The proteins that are precipitated by the b-isox chemical despite treatment of the lysates with RNase are even more enriched in LC sequences than the group of proteins precipitated from untreated lysates. These observations are consistent with the hypothesis that LC sequences directly endow RNA-binding proteins with susceptibility to b-isox-mediated precipitation. By extension, we hypothesize that it is precisely these sequences that also endow RNA-binding proteins with the capacity to reversibly enter and exit RNA granules. This is not to say, however, that RNA is not required for the formation of RNA granules in living cells. The work of Dundr and colleagues has provided evidence that tethered RNA-binding proteins or tethered RNA can prompt the formation of subnuclear bodies (Kaiser et al., 2008; Shevtsov and Dundr, 2011).

Perhaps the most surprising observation reported herein is the ability of hydrogel droplets composed solely of mCherry linked to the LC domain of FUS to recruit and trap the exact same mRNPs that were precipitated by the b-isox chemical. We emphasize the fact that the only polypeptide sequences of FUS present in these hydrogel droplets are those limited to its N-terminal LC domain and that all of the C-terminal RNA-binding domains of FUS are absent in the mCherry:FUS hybrid. The correlation of the precipitated-versus-excluded mRNAs, relative to gel-retained-versus-excluded mRNAs, is highly statistically significant for both the mouse brain lysate and U2OS cell lysate experiments. Kato and colleagues (Kato et al., 2012) have shown that mCherry:FUS hydrogel droplets are capable of trapping the LC domains of heterologous RNA-binding proteins. We offer the interpretation that upon incubation with lysates prepared from either mouse brain tissue or human U2OS cells, the mCherry:FUS hydrogel droplets are able recruit and trap hnRNP proteins bearing LC domains. If these proteins are tightly associated with an RNA substrate, the RNA would likewise be expected to be recruited to the hydrogel droplet.

The experimental paradigm of being able to rapidly isolate, sequence, and identify mRNPs poised for incorporation into RNA granules facilitated the beginnings of a computational approach to assign functional specificity to individual RNA-binding proteins. To this end we used an RNAi approach to attenuate the expression of FUS, EWS, and both proteins in cultured U2OS cells. Lysates were prepared from cells modified in these ways, then exposed to the b-isox chemical so that precipitates could be evaluated by RNA-Seq. This led to the identification of mRNAs underrepresented in the b-isox precipitate following knockdown of FUS, EWS, or both proteins. We were encouraged to find that most of the mRNAs underrepresented in the FUS-alone knockdown experiment were also underrepresented when both FUS and EWS were attenuated by shRNA and that most of the mRNAs underrepresented by EWS-alone knockdown were also attenuated in the double knockdown sample. The statistical significance of these two overlapping data sets is exceptionally high (Experimental Procedures).

We recognize the many shortcomings attendant with this method of analysis. First, the degree of shRNA-mediated knockdown of FUS and EWS ranged between roughly 70% and 90% of the normal cellular levels of the two proteins. Second, even if the level of shRNA-mediated knockdown was significant, target mRNAs for these RNA-binding proteins might enter the b-isox precipitate via interactions with entirely different RNA-binding proteins endowed with LC domains. In other words, it cannot be assumed that movement in and out of RNA granules for any given mRNA is dominantly controlled by a single RNA-binding protein. Third, it is probable that upon preparation of cellular lysates, some degree of reassortment of RNA-binding proteins must take place (Mili and Steitz, 2004). Despite these caveats, if valid, this approach should be capable of highlighting the mRNA species that are most uniquely dependent upon FUS or EWS for RNA granule-mediated regulation. Fortuitously, a recent PAR-CLIP study was reported in search of mRNA targets of FUS and EWS (Hoell et al., 2011). Of the 53 mRNAs that were underrepresented either in the FUS and FUS/EWS knockdown trials, or the EWS and FUS/EWS trials, 36 were represented on the list of FUS/EWS PAR-CLIP targets (Hoell et al., 2011). The statistical probability of this degree of overlap corresponds to a p value lower than the 2.2×10^{-16} limit of the computational program utilized in our studies. As such, we offer the conclusion that the functional approach we have used to identify FUS and EWS target mRNAs helps validate the data set reported by Tuschl and colleagues (Hoell et al., 2011), and that their PAR-CLIP data similarly cross-validate the observations reported herein.

We close by comparing and contrasting the way we conceptualize the utility of LC sequences in the context of RNA regulation with previous studies of prion-like fibrous aggregates. Grappling with the perplexing, non-Mendelian patterns of inheritance of certain strains of yeast (Cox et al., 1988), Wickner (1994) discovered that the [PSI+] and [URE3] strains could infrequently cycle between states wherein the products of these genes would exist as either inactive, prion-like fibers or soluble, functionally

active polypeptides. Extending from this work, Lindquist and colleagues (True and Lindquist, 2000) have argued that fungi profit from the ability of being able to phenotypically alternate between these states. Indeed, Lindquist and Kandel have extended this concept to hypothesize that the permanence of memory may be attributable to the formation of irreversibly polymerized, prion-like aggregates of the CPEB gene product of *Aplysia californica* (Shorter and Lindquist, 2005; Si et al., 2010, 2003). More recently, the Lindquist laboratory has provided compelling evidence that many different yeast proteins are able to be converted into permanently aggregated, prion-like structures (Alberti et al., 2009).

The polypeptide domains required for the formation of the aforementioned yeast and *Aplysia* prions are typified, without exception, by LC sequences indistinguishable from those we have found to be both necessary and sufficient for: (1) reversible precipitation by the b-isox chemical; (2) formation of hydrogels; (3) trapping of otherwise soluble proteins by preformed hydrogel droplets; (4) copolymerization of otherwise soluble proteins into preformed, amyloid-like fibers; and (5) the addressing of RNA-binding proteins to RNA granules. There is no question that these LC domains can enter into irreversible fibrous aggregates, just as happens with the LC domains housed within many gene products associated with neurodegenerative disease (Koyano et al., 1999; Kwiatkowski et al., 2009; Neumann et al., 2006; Vance et al., 2009). We extend this thinking to offer the interpretation that LC sequences can actually exist in one of three states; one being soluble, a second being dynamically reversible with respect to polymeric state, and a third being irreversibly aggregated. We further hypothesize that the first and second of these states represent the underlying biological utility of LC domains, allowing proteins to dynamically move into and out of subcellular compartments that are not membrane bound. We offer the interpretation that LC sequences are conserved evolutionarily for these purposes at the expense of infrequent events leading to irreversible, pathogenic aggregation. Now that it is possible to generate reversible polymers derived from LC sequences, it should be possible to utilize structural approaches to define the differences between the reversibly polymeric, amyloid-like fibers described by Kato and colleagues (Kato et al., 2012) and the irreversible, prion-like aggregates found in studies of both model organisms and human disease.

In order for the observations of this and the accompanying manuscript to be of biological significance, the amyloid-like fibers we describe must be dynamically reversible. That the fibers described in these two papers are far less stable than prion-like amyloids has been confirmed in a variety of ways (Kato et al., 2012). What processes might be used in cells to regulate fiber formation and de-polymerization? In a neuron, for example, why is it that neuronal granules form in the soma, persist during dendritic transport, yet dissolve upon reaching the "oasis" in the vicinity of a synapse? Having found that phosphorylation of the LC domain of FUS by DNA-PK inhibits its retention by mCherry:FUS hydrogel droplets, we offer the speculation that the dynamics of fiber assembly/disassembly might be regulated by posttranslational modification. Perhaps the locale of synapses is enriched in activated protein kinases? Alternatively, other sorts of modification, including acetylation, methylation, or modification by O-GlnNAc sugars might regulate the dynamics of RNA granules. Having distilled a part of the process down to defined biochemical reactions (hydrogel retention and microscopic evidence of fiber polymerization from preexisting seeds), it is hoped that these observations will offer the opportunity to dig deep into the detailed processes used by cells to regulate localized translation.

EXPERIMENTAL PROCEDURES

Computational Analysis of Low Complexity Sequences and *Pumilio* Motif

Low complexity sequences were identified using the SEG program with default parameter settings (Wootton and Federhen, 1996). The length of the longest continuous low complexity segment was calculated for each protein, and proteins with lengths of at least 35 amino acids were considered to have a low complexity domain, selected as the cutoff value as described in Kato et al. (2012). Fisher's exact test using the "R" software (R Development Core Team, 2010) was used to determine whether any set of proteins was enriched with polypeptides containing LC domains compared with the statistics of the mouse and human proteomes. mRNA and 3′ UTR sequences of b-isox pellet- and supernatant-enriched RNAs were analyzed for the pumilio-binding motif 5′-UGUANAUA-3′. Fisher's Exact test using the "R" software was used to determine whether any set of RNAs was enriched with RNAs containing at least one pumilio motif compared with the statistics of the mouse and human transcriptomes.

Hydrogel Retention Assay

To form the mCherry:FUS hydrogels, the purified FUS214 fragment linked to mCherry was dialyzed against a gelation buffer containing 20 mM Tris-HCl (pH 7.5), 200 mM NaCl, 20 mM BME, 0.5 mM EDTA, and 0.1 mM phenylmethylsulfonyl fluoride (PMSF) overnight. The dialyzed protein was concentrated to roughly 60 mg/ml and sonicated 10 s at 12% power on a Fisher Scientific Sonic Dismembrater Model 500. After centrifugation, 0.5 μl droplets of the supernatant were deposited onto a glass-bottomed microscope dish (MatTek, MA, USA). The dish was sealed with parafilm, incubated overnight at room temperature, and aliquoted in 0.5 μl drops into a fluidic chamber to preform into gel. For the MS2 gel retention assay, 2 μM CFP-tagged constructs were incubated with 1 μM Cy5.5 hairpin RNA in gel shift buffer for 30 min on ice. The protein-RNA mixture was then added to the mCherry-FUS214 gel droplet and allowed to equilibrate overnight at 4°C. Horizontal sections of the soaked hydrogel droplets were scanned with both the mCherry and Cy5.5 excitation wavelengths on a Zeiss LSM510 or Leica TCS SP5 confocal microscopes. The images were made by the program ImageJ (NIH, USA).

For incubation with cell lysate, 25 μl mCherry-FUS214 gel droplets were preformed as described above. Ten droplets were incubated for 2 hr at 4°C with 5 ml of lysate prepared from either mouse brain or cultured U2OS cells. Droplets were then spun down at 3,000 × *g* for 5 min, washed twice with PBS, and melted in RNA-Stat for RNA purification. RNA was also isolated from the remaining, gel-excluded lysate. Both fractions were then used to make cDNA libraries for RNA-Seq.

MS2 Gel Shift

MS2 substrate RNA 5′-UAGAAAACAUGAGGAUCACCCAUGUCUGCAG-3′ was synthesized with either 6-FAM covalently linked to the 3′ end or Cy5.5 covalently linked to the 5′ end (IDT, Coralville, IA, USA). Hairpin RNA was prepared by denaturing at 70°C for 5 min then cooling down for 1 min to allow folding. For gel shift assays, 2uM CFP-tagged constructs were incubated with 1 μM 6-FAM-labeled RNA in gel shift buffer containing 20 mM Tris-HCl (pH 7.5), 50 mM KCl, 5 mM $MgCl_2$, 0.5% NP-40, 20 mM BME, 1:500 RNasin, and 0.25 mg/mL yeast tRNA for 30 min on ice. 6× DNA loading dye was added to the protein-RNA mixture and the reaction was run on 5% native acrylamide gel at 120V for 1.5 hr. The gel was then scanned on a Typhoon scanner using the Cy2 filter to detect the 6-FAM signal.

Lentiviral shRNA-Mediated Knockdown

GIPz lentivirus shRNAmir constructs to knockdown FUS and EWS were obtained from Open Biosystems (Thermo Scientific, Waltham, MA, USA). For FUS, the shRNA sequence used was 5′-AGGATAATTCAGACAACAA-3′ catalog number V3LMM_450383 and for EWS, the shRNA sequence used was 5′-AGCAGAGTAGCTATGGTCA-3′ catalog number V3LHS_376291. To generate lentivirus, near confluent 10 cm plates of HEK293FT cells were transiently transfected with 5 μg of pGIPz shRNA construct each and 5 μg viral packaging vectors (1.6 μg pMD2.G, 2.3 μg psPAX2) with 10 μl lipofectamine 2000 (Invitrogen) in Opti-MEM. Media were replaced with DMEM with 10% FBS after 6 hr of transfection and collected 36 hr after transfection. The viral media were filtered through 0.45 μm low protein-binding filter and 10 μg/ml polybrene was added. For viral transduction, 5 ml of viral media and 5 ml of Opti-MEM were added to confluent 15 cm plates of U2OS cells. Transduction efficiency was confirmed by the presence of GFP-positive cells. Knockdown efficiency was confirmed by both qPCR (see Extended Experimental Procedures for primer sequences) and western blotting using rabbit polyclonal antibodies for FUS catalog number A300-294A and EWS catalog number A300-417A (Bethyl Labs, Montgomery, TX, USA).

DNA-PK Phosphorylation Assays

The GFP-FUS LC domain was phosphorylated by human DNA-PK in a 50 μl reaction mixture containing 40 mM HEPES (pH 7.4), 100 mM KCl, 10 mM MgCl 2, 10 ng/μl salmon sperm DNA, 0.2 mM EGTA, 0.1 mM EDTA, 1 mM DTT, 0.1 mM PMSF, 200 μM [γ-^{32}P] ATP, 20 μM GFP-FUS LC domain, and the indicated units of DNA-PK. The reaction mixtures were incubated at 37°C for 1 hr followed by SDS-PAGE and autoradiography. For hydrogel-binding assay, cold ATP was used instead of [γ-^{32}P]ATP. The reaction mixture was 20-fold diluted with the gelation buffer and placed in the mCherry-FUS hydrogel dish. After incubation of 3 days at 4°C, fluorescent images of the GFP signal were retrieved by confocal microscopy.

Proteomic Analysis of DNA-PK-Mediated Phosphorylation

Fifty microliter aliquots of 10 μM FUS protein stock solution treated with increasing amounts of DNA-dependent protein kinase (DNA-PK) were precipitated with 20% TCA followed by a cold acetone wash. Dried proteins were reduced by adding 5 mM DTT and incubation at 37°C for 30 min. Proteins were then alkylated by exposure to 10 mM iodoacetamide for 30 min at room temperature. Samples were then diluted 8-fold using 100 mM Tris (pH 8.0), 10 mM $CaCl_2$ and urea supplemented to a final concentration of 1M. Proteins were then digested with chymotrypsin for 18 hr at 37°C, separated on a C18 reversed-phase column and eluted directly into a LTQ Oribitrap Velos mass spectrometer. Quantitation of FUS phosphor-site containing peptides was performed by manual integration of MS extracted ion chromatograms using Xcalibur version 2.1, Thermo Scientific. Corrected chromatographic peaks for quantitation were identified by matching to the accurate mass and retention time of a confident peptide identification from MS/MS spectra in at least one of the data files. Raw data files were processed using the Mascot workflow in Proteome Discoverer using default parameters. Identified peptides containing the phosphorylation sites described by Gardiner and colleagues (2008), and a Mascot score of at least 30, were manually inspected. The m/z and retention times were then used for quantitation of the peptide across the data sets by extracting ion chromatogram (XIC) as described above.

SUPPLEMENTAL INFORMATION

Supplemental Information includes Extended Experimental Procedures and five tables and can be found with this article online at doi:10.1016/j.cell.2012.04.016.

ACKNOWLEDGMENTS

We thank Mike Rosen, Randal Halfmann, and Michael Dambach for valuable input; Joan Steitz, Geraldine Sedoux, Joe Gall, Ben Tu, Mike Rosen, and Phil Sharp for helpful criticisms of the manuscript; and the shared resource cores in Proteomics and DNA Sequencing at UTSWMC for technical support. This work was funded by an unrestricted endowment provided S.L.M. by an anonymous donor.

Received: January 5, 2012
Revised: March 22, 2012
Accepted: April 24, 2012
Published: May 10, 2012

REFERENCES

Alberti, S., Halfmann, R., King, O., Kapila, A., and Lindquist, S. (2009). A systematic survey identifies prions and illuminates sequence features of prionogenic proteins. Cell *137*, 146–158.

Bernardi, A., and Spahr, P.F. (1972). Nucleotide sequence at the binding site for coat protein on RNA of bacteriophage R17. Proc. Natl. Acad. Sci. USA *69*, 3033–3037.

Böckers, T.M., Segger-Junius, M., Iglauer, P., Bockmann, J., Gundelfinger, E.D., Kreutz, M.R., Richter, D., Kindler, S., and Kreienkamp, H.J. (2004). Differential expression and dendritic transcript localization of Shank family members: identification of a dendritic targeting element in the 3′ untranslated region of Shank1 mRNA. Mol. Cell. Neurosci. *26*, 182–190.

Bramham, C.R., and Wells, D.G. (2007). Dendritic mRNA: transport, translation and function. Nat. Rev. Neurosci. *8*, 776–789.

Burgin, K.E., Waxham, M.N., Rickling, S., Westgate, S.A., Mobley, W.C., and Kelly, P.T. (1990). In situ hybridization histochemistry of Ca2+/calmodulin-dependent protein kinase in developing rat brain. J. Neurosci. *10*, 1788–1798.

Caceres, A., Payne, M.R., Binder, L.I., and Steward, O. (1983). Immunocytochemical localization of actin and microtubule-associated protein MAP2 in dendritic spines. Proc. Natl. Acad. Sci. USA *80*, 1738–1742.

Cox, B.S., Tuite, M.F., and McLaughlin, C.S. (1988). The psi factor of yeast: a problem in inheritance. Yeast *4*, 159–178.

Feng, Y., Gutekunst, C.A., Eberhart, D.E., Yi, H., Warren, S.T., and Hersch, S.M. (1997). Fragile X mental retardation protein: nucleocytoplasmic shuttling and association with somatodendritic ribosomes. J. Neurosci. *17*, 1539–1547.

Gardiner, M., Toth, R., Vandermoere, F., Morrice, N.A., and Rouse, J. (2008). Identification and characterization of FUS/TLS as a new target of ATM. Biochem. J. *415*, 297–307.

Grooms, S.Y., Noh, K.M., Regis, R., Bassell, G.J., Bryan, M.K., Carroll, R.C., and Zukin, R.S. (2006). Activity bidirectionally regulates AMPA receptor mRNA abundance in dendrites of hippocampal neurons. J. Neurosci. *26*, 8339–8351.

Hegner, R.W. (1908). Effects of removing the germ-cell determinants from the eggs of some chrysomelid beetles. Preliminary report. Biol. Bull. *16*, 19–26.

Hegner, R.W. (1911). Experiments with chrysomelid beetles. III. The effects of killing parts of the eggs of Leptinotarsa decemlineata. Biol. Bull. *20*, 237–251.

Herb, A., Wisden, W., Catania, M.V., Maréchal, D., Dresse, A., and Seeburg, P.H. (1997). Prominent dendritic localization in forebrain neurons of a novel mRNA and its product, dendrin. Mol. Cell. Neurosci. *8*, 367–374.

Hoell, J.I., Larsson, E., Runge, S., Nusbaum, J.D., Duggimpudi, S., Farazi, T.A., Hafner, M., Borkhardt, A., Sander, C., and Tuschl, T. (2011). RNA targets of wild-type and mutant FET family proteins. Nat. Struct. Mol. Biol. *18*, 1428–1431.

Illmensee, K., and Mahowald, A.P. (1974). Transplantation of posterior polar plasm in Drosophila. Induction of germ cells at the anterior pole of the egg. Proc. Natl. Acad. Sci. USA *71*, 1016–1020.

Kaiser, T.E., Intine, R.V., and Dundr, M. (2008). De novo formation of a subnuclear body. Science *322*, 1713–1717.

Kato, M., Han, T.W., Xie, S., Shi, K., Du, X., Wu, L.C., Mirzaei, H., Goldsmith, E.J., Longgood, J., and Pei, J. (2012). Cell-Free Formation of RNA Granules: Low Complexity Sequence Domains Form Dynamic Fibers within Hydrogels. Cell *149*, this issue, 753–767.

Kislauskis, E.H., Li, Z., Singer, R.H., and Taneja, K.L. (1993). Isoform-specific 3′-untranslated sequences sort alpha-cardiac and beta-cytoplasmic actin messenger RNAs to different cytoplasmic compartments. J. Cell Biol. *123*, 165–172.

Kislauskis, E.H., Zhu, X., and Singer, R.H. (1994). Sequences responsible for intracellular localization of beta-actin messenger RNA also affect cell phenotype. J. Cell Biol. *127*, 441–451.

Knowles, R.B., Sabry, J.H., Martone, M.E., Deerinck, T.J., Ellisman, M.H., Bassell, G.J., and Kosik, K.S. (1996). Translocation of RNA granules in living neurons. J. Neurosci. *16*, 7812–7820.

Koyano, S., Uchihara, T., Fujigasaki, H., Nakamura, A., Yagishita, S., and Iwabuchi, K. (1999). Neuronal intranuclear inclusions in spinocerebellar ataxia type 2: triple-labeling immunofluorescent study. Neurosci. Lett. *273*, 117–120.

Kuhl, D., and Skehel, P. (1998). Dendritic localization of mRNAs. Curr. Opin. Neurobiol. *8*, 600–606.

Kwiatkowski, T.J., Jr., Bosco, D.A., Leclerc, A.L., Tamrazian, E., Vanderburg, C.R., Russ, C., Davis, A., Gilchrist, J., Kasarskis, E.J., Munsat, T., et al. (2009). Mutations in the FUS/TLS gene on chromosome 16 cause familial amyotrophic lateral sclerosis. Science *323*, 1205–1208.

Lehmann, R., and Nusslein-Volhard, C. (1987). Involvement of the pumilio gene in the transport of an abdominal signal in the Drosophila embryo. Nature *329*, 167–170.

Link, W., Konietzko, U., Kauselmann, G., Krug, M., Schwanke, B., Frey, U., and Kuhl, D. (1995). Somatodendritic expression of an immediate early gene is regulated by synaptic activity. Proc. Natl. Acad. Sci. USA *92*, 5734–5738.

Lyford, G.L., Yamagata, K., Kaufmann, W.E., Barnes, C.A., Sanders, L.K., Copeland, N.G., Gilbert, D.J., Jenkins, N.A., Lanahan, A.A., and Worley, P.F. (1995). Arc, a growth factor and activity-regulated gene, encodes a novel cytoskeleton-associated protein that is enriched in neuronal dendrites. Neuron *14*, 433–445.

Mahowald, A.P. (1962). Fine structure of pole cells and polar granules in Drosophila melanogaster. J. Exp. Zool. *151*, 201–215.

Mili, S., and Steitz, J.A. (2004). Evidence for reassociation of RNA-binding proteins after cell lysis: implications for the interpretation of immunoprecipitation analyses. RNA *10*, 1692–1694.

Miller, S., Yasuda, M., Coats, J.K., Jones, Y., Martone, M.E., and Mayford, M. (2002). Disruption of dendritic translation of CaMKIIalpha impairs stabilization of synaptic plasticity and memory consolidation. Neuron *36*, 507–519.

Mortazavi, A., Williams, B.A., McCue, K., Schaeffer, L., and Wold, B. (2008). Mapping and quantifying mammalian transcriptomes by RNA-Seq. Nat. Methods *5*, 621–628.

Muddashetty, R.S., Kelić, S., Gross, C., Xu, M., and Bassell, G.J. (2007). Dysregulated metabotropic glutamate receptor-dependent translation of AMPA receptor and postsynaptic density-95 mRNAs at synapses in a mouse model of fragile X syndrome. J. Neurosci. *27*, 5338–5348.

Murata, Y., and Wharton, R.P. (1995). Binding of pumilio to maternal hunchback mRNA is required for posterior patterning in Drosophila embryos. Cell *80*, 747–756.

Neumann, M., Sampathu, D.M., Kwong, L.K., Truax, A.C., Micsenyi, M.C., Chou, T.T., Bruce, J., Schuck, T., Grossman, M., Clark, C.M., et al. (2006). Ubiquitinated TDP-43 in frontotemporal lobar degeneration and amyotrophic lateral sclerosis. Science *314*, 130–133.

Nover, L., Scharf, K.D., and Neumann, D. (1983). Formation of cytoplasmic heat shock granules in tomato cell cultures and leaves. Mol. Cell. Biol. *3*, 1648–1655.

Okada, M., Kleinman, I.A., and Schneiderman, H.A. (1974). Restoration of fertility in sterilized Drosophila eggs by transplantation of polar cytoplasm. Dev. Biol. *37*, 43–54.

Palacios, I.M., and St Johnston, D. (2001). Getting the message across: the intracellular localization of mRNAs in higher eukaryotes. Annu. Rev. Cell Dev. Biol. *17*, 569–614.

R Development Core Team. (2010). R: A language and environment for statistical computing (Vienna, Austria: R Foundation for Statistical Computing).

Shevtsov, S.P., and Dundr, M. (2011). Nucleation of nuclear bodies by RNA. Nat. Cell Biol. *13*, 167–173.

Shorter, J., and Lindquist, S. (2005). Prions as adaptive conduits of memory and inheritance. Nat. Rev. Genet. *6*, 435–450.

Si, K., Lindquist, S., and Kandel, E.R. (2003). A neuronal isoform of the aplysia CPEB has prion-like properties. Cell *115*, 879–891.

Si, K., Choi, Y.B., White-Grindley, E., Majumdar, A., and Kandel, E.R. (2010). Aplysia CPEB can form prion-like multimers in sensory neurons that contribute to long-term facilitation. Cell *140*, 421–435.

Trapnell, C., Pachter, L., and Salzberg, S.L. (2009). TopHat: discovering splice junctions with RNA-Seq. Bioinformatics *25*, 1105–1111.

Trapnell, C., Williams, B.A., Pertea, G., Mortazavi, A., Kwan, G., van Baren, M.J., Salzberg, S.L., Wold, B.J., and Pachter, L. (2010). Transcript assembly and quantification by RNA-Seq reveals unannotated transcripts and isoform switching during cell differentiation. Nat. Biotechnol. *28*, 511–515.

True, H.L., and Lindquist, S.L. (2000). A yeast prion provides a mechanism for genetic variation and phenotypic diversity. Nature *407*, 477–483.

Vance, C., Rogelj, B., Hortobágyi, T., De Vos, K.J., Nishimura, A.L., Sreedharan, J., Hu, X., Smith, B., Ruddy, D., Wright, P., et al. (2009). Mutations in FUS, an RNA processing protein, cause familial amyotrophic lateral sclerosis type 6. Science *323*, 1208–1211.

Vessey, J.P., Schoderboeck, L., Gingl, E., Luzi, E., Riefler, J., Di Leva, F., Karra, D., Thomas, S., Kiebler, M.A., and Macchi, P. (2010). Mammalian Pumilio 2 regulates dendrite morphogenesis and synaptic function. Proc. Natl. Acad. Sci. USA *107*, 3222–3227.

Wang, H., Kunkel, D.D., Schwartzkroin, P.A., and Tempel, B.L. (1994). Localization of Kv1.1 and Kv1.2, two K channel proteins, to synaptic terminals, somata, and dendrites in the mouse brain. J. Neurosci. *14*, 4588–4599.

Wickner, R.B. (1994). [URE3] as an altered URE2 protein: evidence for a prion analog in Saccharomyces cerevisiae. Science *264*, 566–569.

Wootton, J.C., and Federhen, S. (1996). Analysis of compositionally biased regions in sequence databases. Methods Enzymol. *266*, 554–571.

Ye, B., Petritsch, C., Clark, I.E., Gavis, E.R., Jan, L.Y., and Jan, Y.N. (2004). Nanos and Pumilio are essential for dendrite morphogenesis in Drosophila peripheral neurons. Curr. Biol. *14*, 314–321.

Zamore, P.D., Williamson, J.R., and Lehmann, R. (1997). The Pumilio protein binds RNA through a conserved domain that defines a new class of RNA-binding proteins. RNA *3*, 1421–1433.

Zhang, B., Gallegos, M., Puoti, A., Durkin, E., Fields, S., Kimble, J., and Wickens, M.P. (1997). A conserved RNA-binding protein that regulates sexual fates in the C. elegans hermaphrodite germ line. Nature *390*, 477–484.

Zhang, H.L., Eom, T., Oleynikov, Y., Shenoy, S.M., Liebelt, D.A., Dictenberg, J.B., Singer, R.H., and Bassell, G.J. (2001). Neurotrophin-induced transport of a beta-actin mRNP complex increases beta-actin levels and stimulates growth cone motility. Neuron *31*, 261–275.